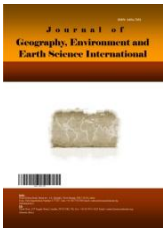

Journal of Geography, Environment and Earth Science International

25(9): 1-18, 2021; Article no.JGEESI.73468
ISSN: 2454-7352

Bouguer Anomaly of Geothermal Reservoir at Tiris Area, Probolinggo, East Java, Indonesia

Salman Hamja Siombone[1*], Sukir Maryanto[2] and Wiyono[3]

[1]Department of Mathematics and Natural Science Education, STKIP Gotong-Royong, Trans Seram Street, Masohi, Moluccas, Indonesia.
[2]Volcanology and Geothermal Research, University of Brawijaya, Veteran Street, Malang, East Java, Indonesia.
[3]Department of Physics, Faculty of Mathematics and Natural Science, University of Brawijaya, Veteran Street, Malang, East Java, Indonesia.

Authors' contributions

This work was carried out in collaboration among all authors. All authors read and approved the final manuscript.

Article Information

DOI: 10.9734/JGEESI/2021/v25i930304
Editor(s):
(1) Dr. Teresa Lopez-Lara, Autonomous University of Queretaro, Mexico.
Reviewers:
(1) Nordiana Mohd Muztaza, Universiti Sains Malaysia, Malaysia.
(2) Ayad Abderrahim, Abdelmalek Essaâdi University, Morocco.
(3) Jianguo Wang, China University of Mining and Technology, China.
Complete Peer review History: https://www.sdiarticle4.com/review-history/73468

Original Research Article

Received 07 July 2021
Accepted 17 September 2021
Published 23 September 2021

ABSTRACT

Research related to the geothermal system in the Tiris geothermal area (TGA) Probolinggo Regency has been conducted using the gravity method. This study aims to investigate the subsurface structure, with a target on estimating geothermal reservoir rocks from the study area. This study utilized the Gravity meter *La Coste & Romberg type G-1503* on 116 acquisition points in an area of 2.16 km^2, covering all geothermal manifestation points in TGA. The gravity measurement data obtained is then processed through gravity corrections, which include: conversion into milli-Gals (mGal) units, tidal correction, drift correction, latitude correction, free air correction, Bouguer correction, and terrain correction. These corrections to obtain a complete Bouguer anomaly (CBA) value. The study area shows the CBA value on a horizontal plane which ranges from 0.1 mGal to 4.2 mGal. The separation of the regional and residual Bouguer anomaly from the CBA on a horizontal plane employed the *Moving Average* method through spectrum analysis. The value of residual Bouguer anomaly ranges from -0.7 mGal to 2.7 mGal. The low anomalies are scattered in

**Corresponding author: E-mail: salmansiombone@gmail.com;*

the northwest, and a small number are spread in the northeast and southeast, while the high anomalies are in the middle of the study area. The result of 3D inversion modeling finds that the study area's subsurface structure consists of four rock layers, namely lapilli tuff, tuffaceous breccia, volcanic breccia, and basalt. Volcanic breccia is approximated as geothermal reservoir rocks at a depth of 700 to 1000 meters below the acquisition point. In contrast, basalt is supposed to be intrusive igneous rock because it tends to break through the surface at a depth of 348 to 350 meters below the acquisition point. The presence of these intrusive rocks can be predicted through spectrum analysis result, which shows a regional anomaly source at a depth of 348 meters below the acquisition point. This intrusion rock is suspected to be a heat source rock in the geothermal system in the study area.

Keywords: Tiris geothermal area; gravity method; geothermal manifestation; complite Bouguer anomaly; geothermal reservoir; intrusive rocks.

1. INTRODUCTION

1.1 Background to the Study

Probolinggo is a regency in East Java, Indonesia, whose geothermal potential appeared around the Lamongan volcano. Based on the Ministry of Energy and Mineral Resources data, geothermal potential around the Lamongan volcano with about 11 km^2 broad is estimated at 74 MWe to 147 MWe [1,2]. One of the potential geothermal locations around the Lamongan volcano appears in the northeast of this area, precisely in the village of Tiris. The potential is characterized by the presence of geothermal manifestations in the form of four hot springs around the Tancak river of Tiris. The surface temperature of the springs ranges from 38°C to 45°C [1,3]. The geothermal potential at Tiris needs to be observed to obtain reservoir description from its geothermal system [4,5]. Investigation on the existence of geothermal potential can be carried out by using the subsurface investigation methods, one of which is the geophysical method.

A geophysical method used to investigate subsurface conditions is the gravity method. The gravity method is employed to measure variations in the gravitational field somewhere below the earth's surface to collect information in the form of local density from a rock formation [6]. This method is very sensitive to vertical changes, so it can be used to describe subsurface geological structures based on the variations of gravitational fields due to differences in lateral density [7]. The description of the geological structure of the rock types below the surface and its distribution both vertically and laterally is indicated by its density value. In the geothermal case, the difference of density becomes the reference in the gravity method investigation. The areas with heat sources and their accumulation below the surface cause differences in the density of the surrounding rock masses [8]. The difference in density of subsurface rock at the location of geothermal manifestations can be shown in the form of a Gravity anomaly distribution (complete Bouguer anomaly/CBA), which will later be used to interpret, and subsequent processes from CBA data be used to estimate subsurface structures. Estimation of subsurface structures can be done by modeling Gravity data and utilizing relevant geological information from the Study area. The utilization of the gravity method to analyze rock density is considered appropriate because this method has a perfect response towards subsurface rock density [5,9]. Because of its exact ability to estimate subsurface conditions, the gravity method is employed for determining the geothermal reservoir in the area of Tiris, Probolinggo, East Java.

1.2 Geological Overview in the Study Area

The village of Tiris (Tiris Geothermal Area/TGA) is located in the subdistrict of Tiris, district of Probolinggo, East Java, Indonesia. Geographically, the TGA is located at zone 49 in the southern hemisphere, with easting: 764405 mE to 762553 mE and northing: 9120226 mS to 9118993 mS. The average altitude of the study area is 539.25 m.a.s.l (meters above sea level), as shown in Fig. 1. Volcanostratigraphically, the Tiris region has two eruption centers from the growth of volcanic activity that occurred in this area. The areas considered to have geothermal prospects are at the top of the Lamongan volcano as an up-flow characterized by the presence of fumaroles and alteration of rocks. At the same time, the outflow zone is estimated to lead to the northeast of the Lamongan volcano

[1]. Geomorphologically, the area around the Lamongan volcano includes two dominant faults in the northwest to the southeast, viz at the Lamongan volcano body and to the northeast of the Lamongan volcano in TGA [4,10], where there is the opening of *graben* structures associated with the Tancak river. The geothermal manifestations are located around the Tancak river lane, precisely in the flood plain area. Tancak river is a river centered in the Argopuro volcano. The hot springs at points 1 and 2 as the geothermal manifestation 1 are at the altitude of 476 m.a.s.l and 480 m.a.s.l, while the hot springs at points 3 and 4 as the geothermal manifestation 2 are at the altitude of 497 m.a.s.l and 490 m.a.s.l. These show that the geothermal manifestations in TGA are generally in an area with lower topography than the surrounding area.

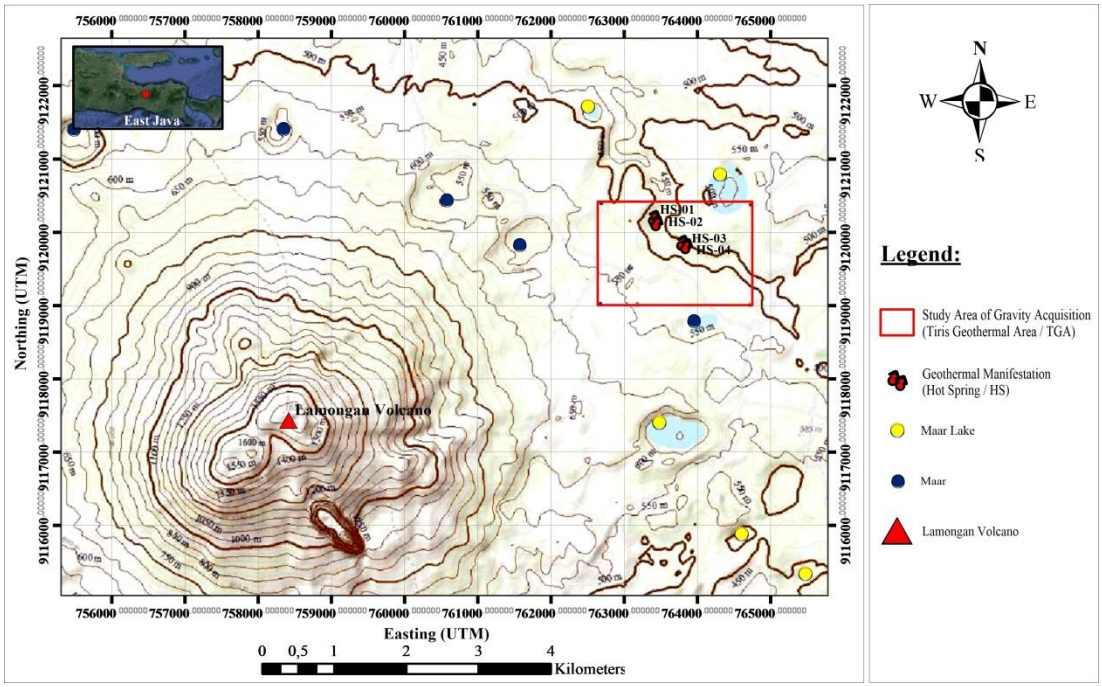

Fig. 1. The geographical location of the study area (TGA) in the northeast of the Lamongan volcano

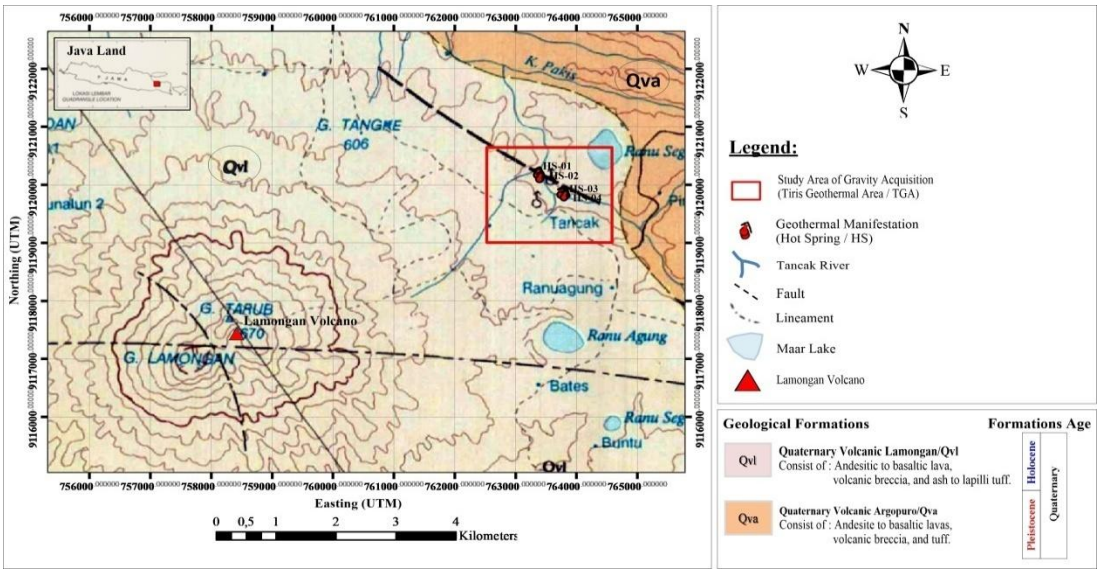

Fig. 2. Geological map of Probolinggo regency and the study area in the northeast of the Lamongan volcano (Modified from [11])

The geological structure that develops in the study area is fracture and fault. The fault and fracture develop well in Argopuro andesitic lava, Lamongan andesitic lava, and morphological lineament in Lamongan-Argopuro pyroclastic flow. The existence of faults in the study area is the lane of hot springs or hot fluids leading to the surface, thus affecting the pattern of alterative distribution and the appearance of hot springs [1,4]. Weak zones around the fault bring out four hot spring points along the Tancak river [3,10]. Based on the geological map of Probolinggo, the study area is in the Lamongan volcanic rock formation (Qvl), which consists of Andesitic to basaltic lava, volcanic breccia, and lapilli tuff. The Qvl formation in the study area is directly adjacent to the Argopuro volcanic formation (Qva). The Qva formation is consists of andesitic to basalt lavas, volcanic breccia, and tuff [11], as shown in Fig. 2.

2. MATERIALS AND METHODS

Gravity measurements in TGA were performed on 116 measuring stations (acquisition points). Data acquisition was carried out by utilizing the Gravity meter *La Coste & Romberg type G-1053* from 18th to 22nd of September 2018. By using this mechanical instrument of gravity, all errors from the data acquisition can be determined from the value of the tool calibration factor [5]. This measurement was carried out around the Tancak river lane of TGA with the study area of 2.16 km^2, as shown in Fig. 3 and Fig. 4. This study was designed in the form of a grid with a distance between the acquisition points of 150 meters. The acquisition points are made into a grid with uniform spacing to make the data from the mapping of subsurface structures at the study area more accurate. The acquisition points grid focuses on estimating the subsurface geological structure of the geothermal manifestation points in the TGA. The base point used in the study area was first determined from the first derivative base point, which has an absolute value, situated behind the Physics Department building, Brawijaya University, Malang.

The gravity data obtained from the measurement were in the form of *counter reading*, so they had to be converted into milli-Gals (mGal) units. After that, the gravity data corrections were performed, including tidal correction, drift correction, latitude correction, free air correction, Bouguer correction, and terrain correction [12,13]. After that, the Bouguer density (local density) was estimated at the study area using the Parasnis method [14,15]. This local density value was used to calculate the complete Bouguer anomaly (CBA). CBA is the difference between the observed gravity value and the theoretical gravity value defined on the observational point and not on the reference spheroid, either ellipsoid or geoid [7]. CBA is obtained by the following equation (1) [6,16]:

$$\Delta g_{BA} = g_{obs} - g_{\varphi} + (\Delta g_{FA} - \Delta g_{B} + \Delta g_{T}) \quad (1)$$

where, Δg_{BA} is CBA (mGal), g_{obs} is the value of gravitational acceleration measured at the measuring station/acquisition point (mGal), g_{φ} is latitude correction (mGal), Δg_{FA} is free air correction, Δg_{B} is Bouguer correction, and Δg_{T} is terrain correction [6]. Latitude correction g_{φ}, free air correction Δg_{FA}, Bouguer correction Δg_{B} and terrain correction Δg_{T} are theoretical gravity values [5,13].

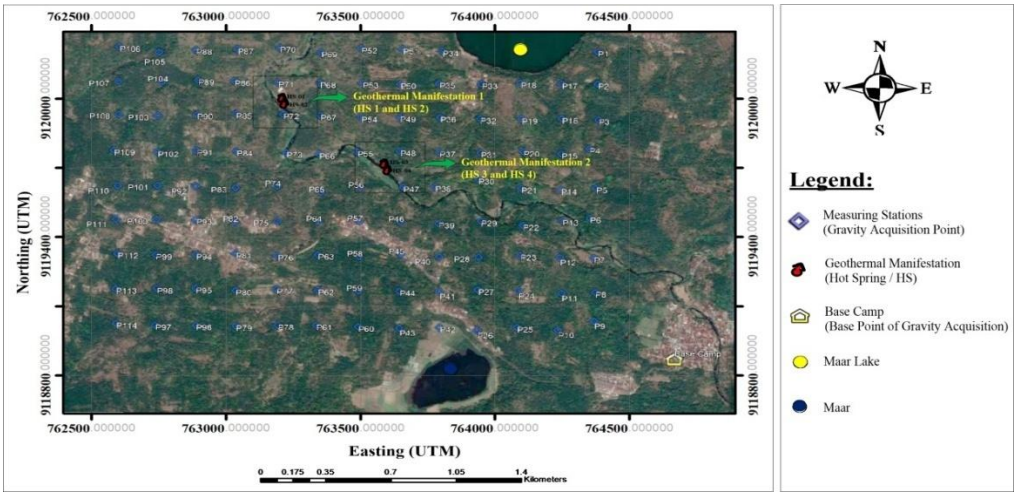

Fig. 3. Gravity acquisition points of the study area

Fig. 4. Gravity Data Acquisition at the study area

Generally, the CBA data are still exposed on the topographic surface of the study area with varying altitudes. The varied altitude of acquisition points can distort the gravity data, so the CBA data must be reduced into a horizontal plane with regular altitude. This reduction process uses a method proposed by Dampney, viz the equivalent source method. The step of the Dampney method is to determine the equivalent source of the discrete point masses at a certain depth below the surface by utilizing CBA data [17,18]. In this method, the equivalent source of the discrete point masses lies on the horizontal plane with depth below the reference spheroid [19]. The optimum depth based on the Dampney experiment must fulfil the following equation (2) [17,18]:

$$g_z(x,y,z) = G\int_{-\infty}^{\infty}\int_{-\infty}^{\infty}\frac{\rho(\alpha,\beta,h)(h-z)d\alpha d\beta}{\{(x-\alpha)^2+(y-\beta)^2+(z-h)^2\}^{3/2}} \quad (2)$$

where, $g_z(x,y,z)$ is the CBA value at point (x, y, z) (mGal), G is the universal gravitational constant (G = 6,674 x 10^{-11} Nm^2. kg^{-2}), $\rho(\alpha,\beta,h)$ is the distribution of surface density contrast that includes z = h, h is the equivalent depth of the point masses on a horizontal plane (meters), x is the longitude coordinate (easting) of the observational point (meters), y is the latitude coordinate (northing) of the observational point (meters), z is an upright axis with a downward direction as a positive value (meters).

The best value of $(h - z)$, based on the results of the Dampney experiment, must fulfill the following equation (3) [17,18]:

$$2.5\,\Delta x < (h - z_i) < 6\Delta x \quad (3)$$

where, Δx is the average distance between observational stations, h is the depth field of the equivalent source of the discrete point masses, and z_i is the height of the observational point.

The separation of regional Bouguer anomaly and residual Bouguer anomaly utilized the *Moving Average* method based on spectrum analysis [20]. Spectrum analysis was performed after the CBA data on a horizontal plane were digitized and then transformed into the frequency domain using Fast Fourier Transform (FFT). FFT of the gravitational anomaly of vertical component F[g_z] on the desired slice line is calculated by the following equation (4) [21]:

$$\mathcal{F}[g_z] = 2\pi G\mu\, e^{|k|(z_0 - z')}\ ; \qquad z' > z_0 \quad (4)$$

where, g_z is the vertical component of gravitational anomaly, k is wave number; z_0 is the elevation of gravity acquisition points on the surface, and z' is the depth of body anomaly in the subsurface. The natural logarithm of the FFT amplitude ($\mathcal{F}[g_z]$) is obtained by the following equation (5) [21]:

$$\text{Ln A} = \text{Ln}\,\mathcal{F}[g_z] = |k|(z_0 - z') \quad (5)$$

Furthermore, The separation of regional and residual anomalies using the moving average method required a single-window width (N). The width was determined from the $k_{[\text{cut-off}]}$ value as the border between the rejection-band and pass-band [20]. It is calculated using the following equation (6):

$$N = \frac{2\pi}{k_{[\text{cut-off}]} - \Delta x} \quad (6)$$

where, N is the width of the single window; $k_{[\text{cut-off}]}$ is the cut-off frequency of regional dan residual anomaly, and Δx is the space interval of gravity data on slice line.

The value of single window width was then used in the filtering process in *Oasis Montaj* using the moving average filter (i.e., *symmetric convolution* mva.5x5 filter). The process resulted in the regional Bouguer anomaly. Then, the residual

anomaly was obtained from reducing the CBA on a horizontal plane with the regional Bouguer anomaly.

After the residual anomaly is obtained, the next step is to create a second vertical derivative (SVD) anomaly map. SVD is the best first step in the gravity data interpretation technique because it can highlight and help resolve the boundary of the gravitational anomaly source from shallow sources [21]. In the wavenumber domain, or Fourier domain, SVD is usually calculated using the following equation (7) [22]:

$$\frac{\partial^2 g_z}{\partial z^2} = F^{-1}(|k|^2); \text{ with } |k|^2 = k_x^{\,2} + k_y^{\,2} \qquad (7)$$

Where, G_z is the Fourier transform of g_z, k_x is the respective wavenumber on the x-axis, k_y is the respective wavenumber on the y-axis, and F^{-1} is the inversion operator of the Fourier transform. The Fourier transform operator used in this SVD method is the Elkins 5x5 matrix filter [7].

The interpretation of the results of data processing was performed qualitatively and quantitatively. The qualitative interpretation was made by describing the distribution of anomalies that exist on the Bouguer Anomaly map (CBA on a horizontal plane, residual Bouguer anomaly, and SVD anomaly). In contrast, the quantitative interpretation was performed by describing the result of local density estimation in the study area using the Parasnis method, spectrum analysis with the Moving Average method, and the result of 3D inversion modeling. Detailed discussion on the subsurface condition of the study area was done by correlating between the qualitative and quantitative interpretations.

3. RESULTS AND DISCUSSION

3.1 Local Density Estimation

The local density shows the average density value of the subsurface constituent rocks in the study area. This local density value was obtained from field observation data using the Parasnis method. This method was based on the minimum correlation of the Bouguer gravity anomaly and Bouguer correction [15], which was then plotted into a linear regression analysis graph [14], as shown in Fig. 5.

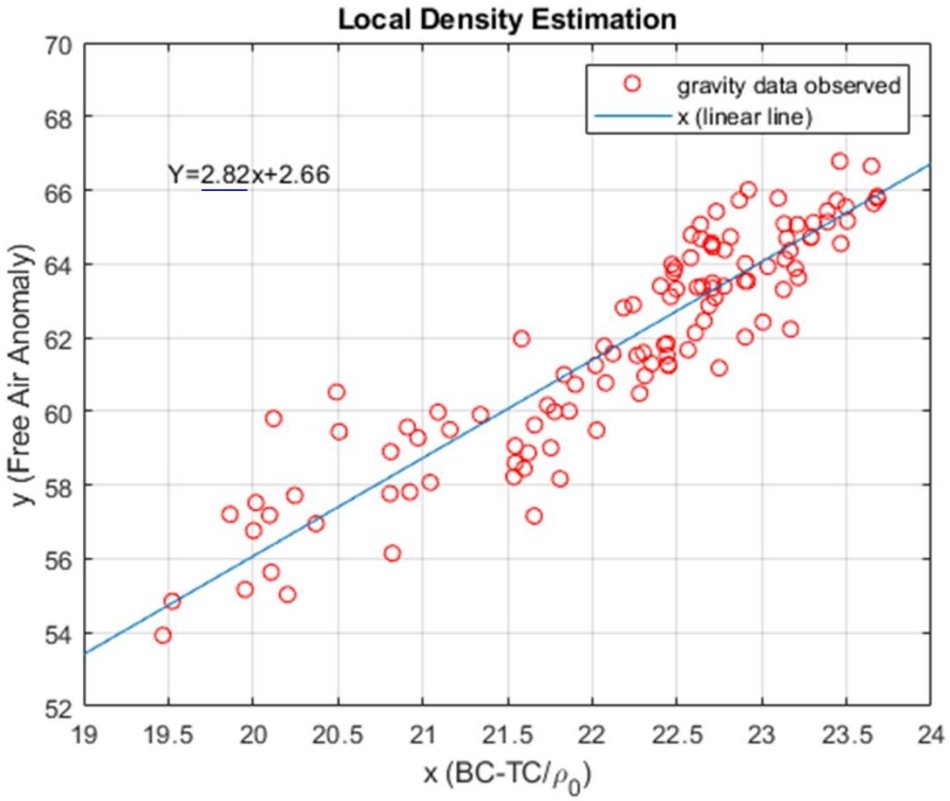

Fig. 5. Estimation of local density at study area using the Parasnis method

Based on the graph of local density estimation in Fig. 5, it is found that the average density at the study area is 2.82 $\mathrm{g/cm^3}$. The density value estimates that the subsurface constituent rocks at the study area are volcanic igneous rocks because they have high-density values. This value positively correlates with the geological information at the study area because it is in the Qvl (Quaternary Volcanic Lamongan) rock formation composed of volcanic igneous rocks [11]. Besides, other supporting data illustrate that the study area has a high-density value, which is indicated by the number of massive rock outcroppings found in the study area. An example of a rock outcrop is shown in Fig. 6.

3.2 Complete Bouguer Anomaly

Complete Bouguer Anomaly (CBA) is a gravitational anomaly obtained from a series of gravity data corrections on each gravity acquisition point, as presented in Fig. 7. Generally, CBA values are spread on the topography of the study area. CBA values are strongly influenced by the density variations laterally in the study area [6]. CBA measured on the surface is a superposition of various sources and the depth of the anomaly below the surface. These various sources are combined events both in the shallow zone (residual) and in the deep zone (regional) [6,23].

Fig. 6. An outcropping of Massive rock at the study area

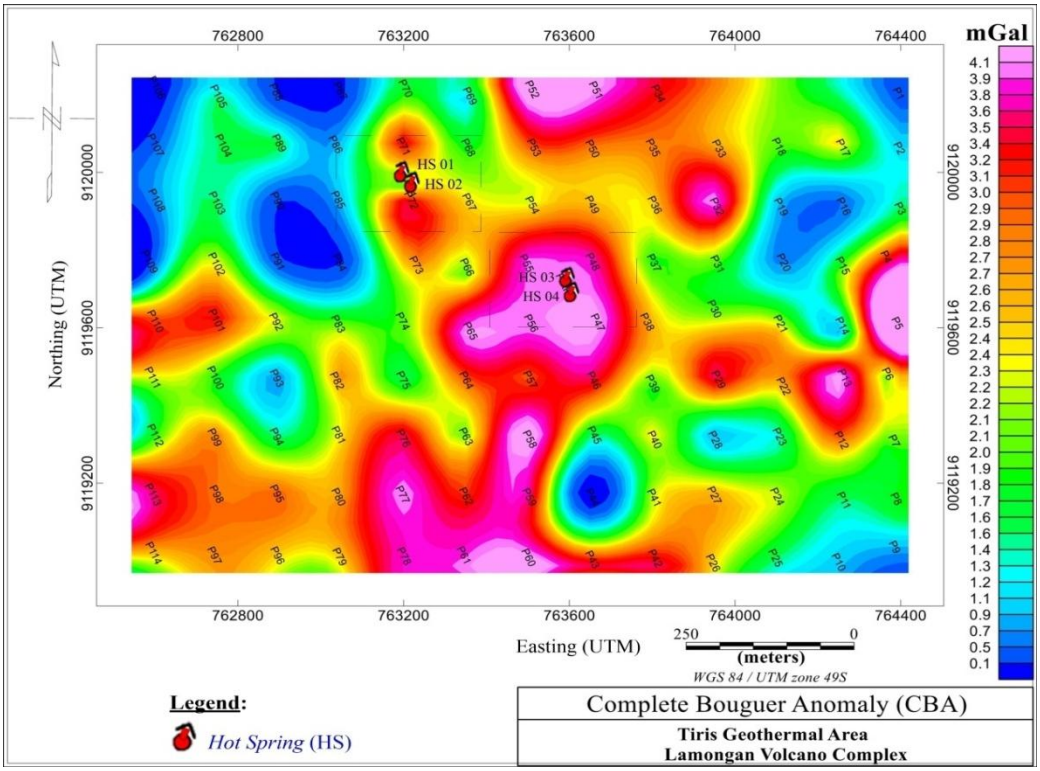

Fig. 7. Complete Bouguer anomaly map of the study area

From the data in Fig. 7, the CBA value ranges from 0.1 mGal to 4.1 mGal. The CBA data are still general because it is a superposition of various events from the influence of regional and residual anomalies, so it cannot be used for further interpretation [24]. For further interpretation, the CBA value must be reduced to a horizontal plane to facilitate the analyzing process of gravity data.

3.3 CBA on a Horizontal Plane

Based on the application of the equivalent source method, the CBA map on a horizontal plane is obtained, as shown in Fig. 8. The application of this method is to minimize distortion so that the obtained gravity data can be used for interpreting subsurface lithological conditions [17,18]. By using this method, the depth of the equivalent source is revealed at 50 meters below the reference spheroid, and the response is calculated at the altitude of 550 meters above the reference spheroid.

Based on the data in Fig. 8, the CBA on a horizontal plane value ranges from 0.1 mGal to 4.2 mGal. CBA value on a horizontal plane is divided into three zones that are low anomaly zone (0.1 mGal to 2.3 mGal), medium anomaly zone (2.4 mGal to 3.0 mGal), and high anomaly zone (3.1 mGal to 4.2 mGal). The value distribution of CBA on a horizontal plane is similar to that of CBA on topography, where low anomaly values are spread more dominantly in the northwest, which is the dominant fault lane. Medium anomalies are associating with high anomalies orient in the middle of the study area. In contrast, high anomalies appear to be more dominant in the middle of the study area from the south to the north. The distribution of this anomaly pattern reflects the subsurface condition of the measurement location [7]. The presence of high anomalies in the middle of the study area indicates that rocks with high-density areas are in this zone with directional orientation in the north to south. Areas with high anomalies generally show subsurface structures that are more compact and denser (high density) than areas with low anomalies [7].

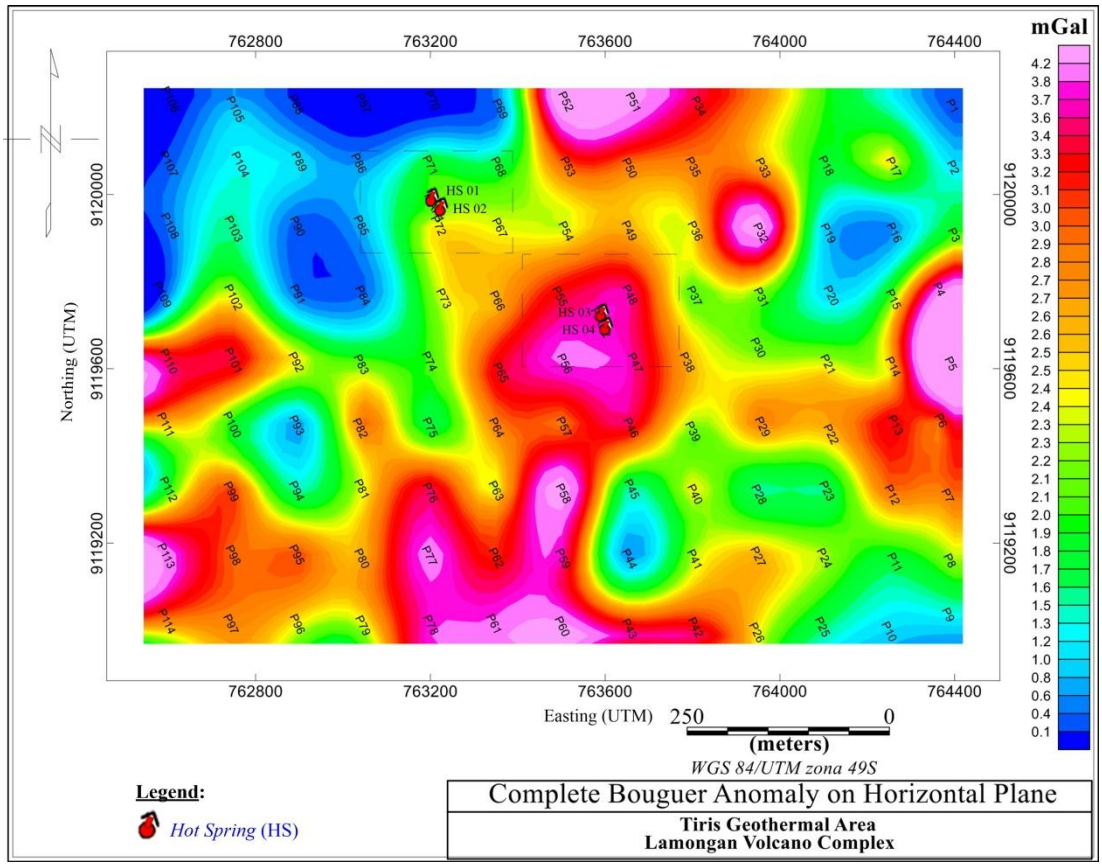

Fig. 8. CBA on a horizontal plane map of the study area

3.4 Spectrum Analysis of Gravity Anomaly

Spectrum analysis was conducted at the map of CBA on a horizontal plane, then 14 slice lines were made. This slice line functions as a moving average for extracting CBA on a horizontal plane data with the digitation method. The digitization data from the 14 slice lines were used for the spectrum analysis process using the Fast Fourier Transform (FFT). The results of spectrum analysis are shown on the graph of the relationship plot between wavenumber (k) and the natural logarithm from FFT amplitude (ln A) (see Fig. 9 and Fig. 10). The spectrum analysis graph can be used to analyze the depth of regional and residual anomalies.

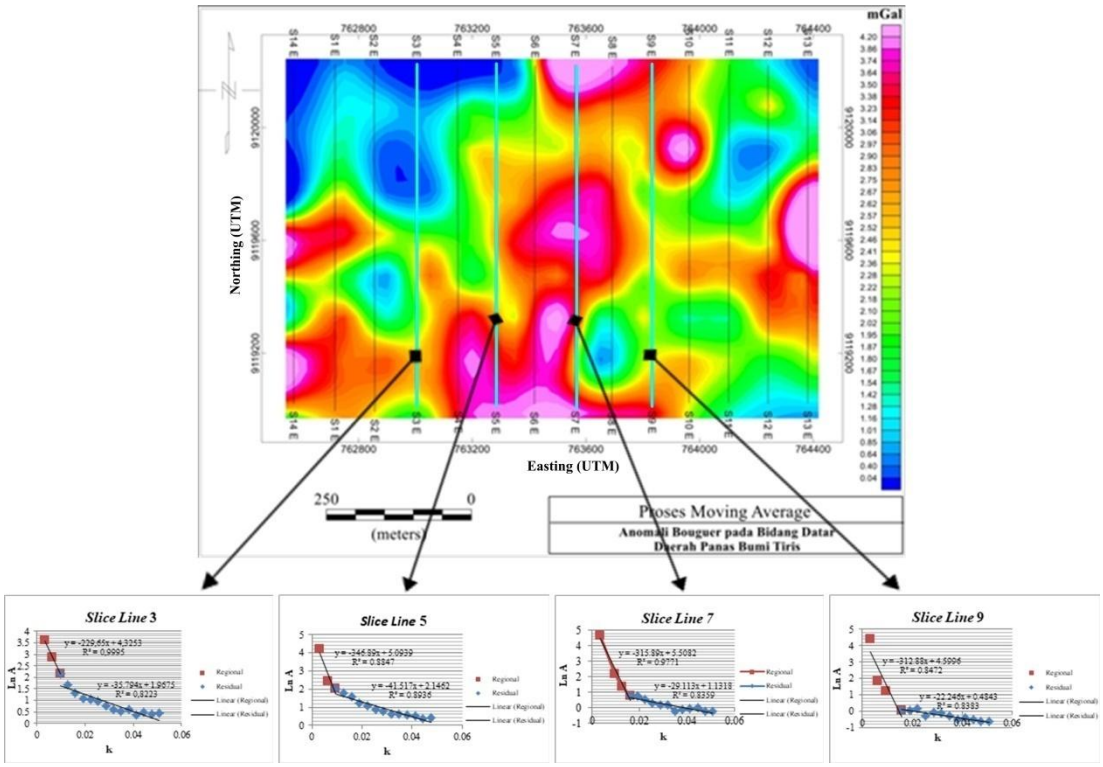

Fig. 9. Moving average process and spectrum analysis of every slice lines

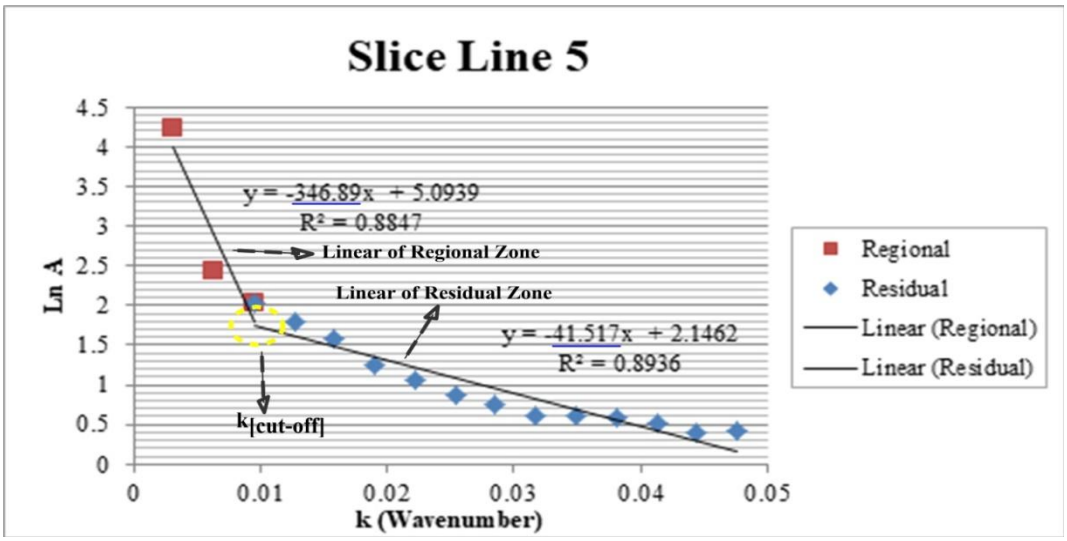

Fig. 10. Spectrum Analysis (k vs ln A) on slice line 5

Fig. 10 shows the results of spectrum analysis from the line slice-5. The figure shows that the depth of the regional anomaly source is 346.89 m below the acquisition point, while the depth of the residual anomaly source is at a shallow depth of 41,52 m below the acquisition point. The depth source of the two anomalies (Fig. 10) only represents line slice-5 and does not represent the entire residual or regional anomaly source from the Study area. In this study, the moving average method is used, which is operated through 14 line slices to thoroughly recap the source data of anomalies in the study area. The regional and residual anomalous depth source data from the 14 line slices are listed in Table 1. The average depth source value of the regional and residual anomalies from the 14 line slices is used to interpret the anomalous depth sources in the Study area.

Based on the results of spectrum analysis, it is obtained that the average depth of the sources of the regional anomaly body is 348 meters below the gravity acquisition point and the average depth of the residual anomaly body is 42 meters below the gravity acquisition point (see Table 1). After obtaining the average depth of the two anomaly sources, the value of the single window width of the 14 data slice lines was determined. Based on the data processing results, the value of the single window width is 19 (see Table 2). Then the window width value was used for the filtering process in the *Oasis Montaj* app using a moving average filter. After the filtering process was carried out, the regional anomaly was obtained.

Based on Table 1, it can be said that the depth of the source of the regional anomaly body originates at a depth of 348 meters below the surface of the study area. Meanwhile, the depth of the source of residual anomaly body originates at a depth of 42 meters below the surface of the study area. The source of this regional anomaly is estimated as a massive body of rocks with a high density near the surface, causing deformation of the rock body above it. Meanwhile, the source of the residual anomaly is supposed to be the result of a breach of high-density rocks underneath, resulting in faults and fractures at shallow depths.

3.5 Regional Bouguer anomaly and residual Bouguer anomaly

The process and the results from the separation of the regional and residual Bouguer anomaly from the CBA on a horizontal plane using the Moving Average method are shown in Fig. 9. The separation of these two anomalies is adjusted to the investigated target for interpretation [25]. Normally, in gravitational surveys, the residual Bouguer anomaly becomes the major concern, and the first step of the interpretation is to eliminate regional effects to isolate residual anomalies [26].

Based on the data in Fig. 11, The regional Bouguer anomaly obtained in the study area ranges from 0.4 mGal to 1.7 mGal. Regional Bouguer anomaly describes the distribution of subsurface rock structures in the very deep layer regionally. In the spectrum analysis process, the average depth of the regional Bouguer anomaly is 348 meters below the study area. This regional Bouguer anomaly cannot be used to model subsurface conditions due to its deep location. Thus, the residual anomaly is needed for the process of modeling and interpretation. Residual anomaly is obtained from reducing the CBA on a horizontal plane with the regional Bouguer anomaly. Residual Bouguer anomalies are shown in Fig. 12.

The residual Bouguer anomaly is the target event in this study because it is related to the effects of superficial mass bodies. Based on the spectrum analysis results, the average depth of the residual anomaly is 42 meters below the study area, so it can be utilized for interpreting shallow subsurface conditions. The residual Bouguer anomaly obtained ranges from -0.7 mGal to 2.6 mGal. This residual Bouguer anomaly value is divided into three zones: low anomaly, medium anomaly, and high anomaly. Low anomalies (-0.7 mGal to 0.9 mGal) are scattered in the northwest (more dominant), and a small portion is spread in the northeast and southeast direction from the study area. At the area with the low anomaly in the northwest of the study area, two hot springs appear at a close distance (geothermal manifestation-1). Medium anomalies (1.0 mGal to 1.5 mGal) are scattered around high and low anomalies in the study area. The high anomaly is in the middle of the study area, which spreads from the south to the north, ranging from 1.5 mGal to 2.7 mGal. On the high anomalies, two hot springs appear, exactly in the middle of the study area (geothermal manifestation-2). This geothermal manifestation-2 is located in an area with a high anomaly, and this condition still causes uncertainty about the existence of weak zones around the area. The shape and boundaries of geological features and fault zones

have not been clearly depicted on the residual Bouguer anomaly map, so a specific approach is needed to overcome it, such as the second vertical derivative (SVD) anomaly map. The exposure for the SVD map will be shown in subheading 3.6.

Table 1. Depth of regional and residual anomalies

No	Depth of regional anomalies (m)	Depth of residual anomalies (m)	C1	C2
1	-207.55	-37.39	4.52	2.03
2	-298.85	-41.61	4.46	1.86
3	-229.65	-35.79	4.33	1.97
4	-280.72	-38.96	4.53	2.40
5	-346.89	-41.52	5.09	2.15
6	-339.72	-38.97	5.11	1.00
7	-315.89	-29.11	5.51	1.13
8	-383.67	-39.90	5.76	2.07
9	-312.88	-22.25	4.60	0.48
10	-720.27	-76.50	6.69	2.36
11	-357.56	-63.00	4.97	1.10
12	-483.65	-42.07	5.76	1.36
13	-430.77	-47.97	6.07	2.20
14	-168.25	-32.47	4.11	1.94
Average	-348.31	-41.96		
Rounding Value	-348	-42		

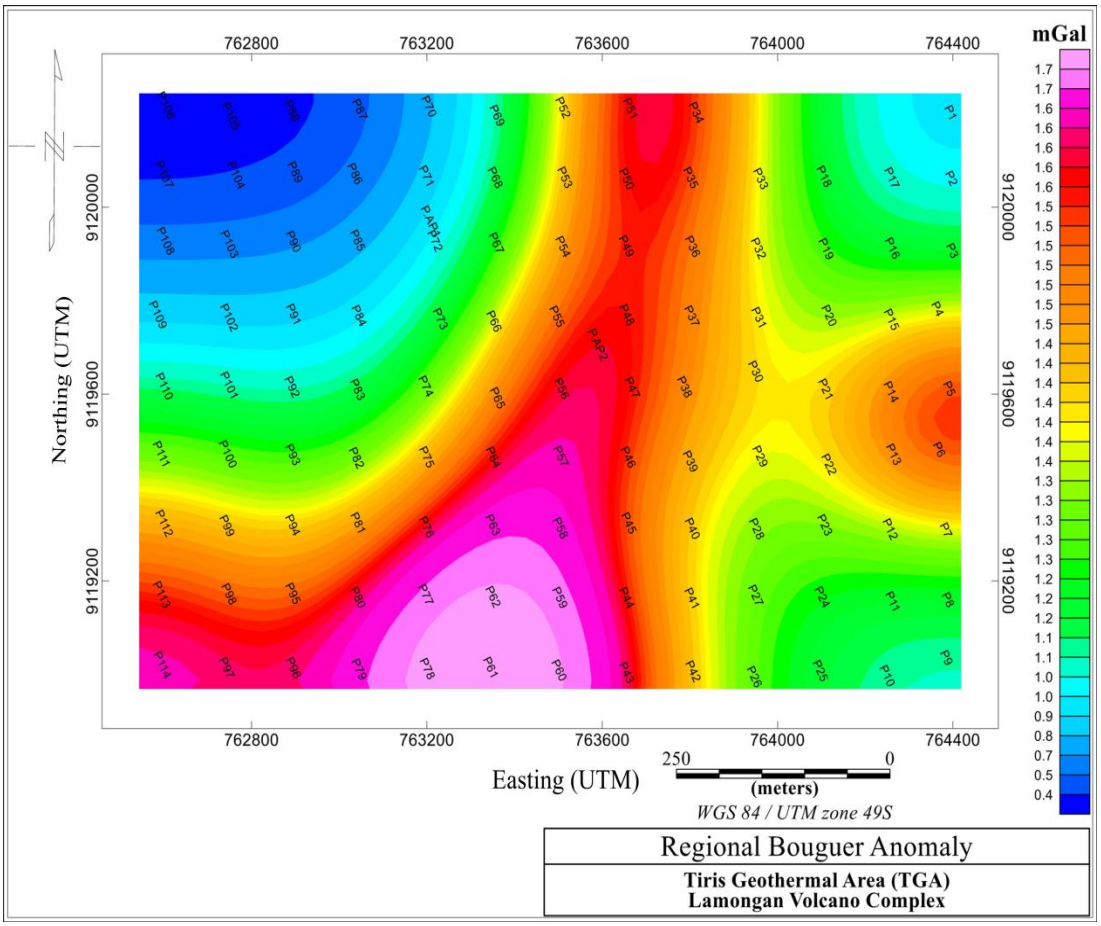

Fig. 11. Regional Bouguer anomaly map of the study area

Tabel 2. Width of single window

x ($k_{[\mathbf{cut-off}]}$)	Lambda (λ)	$\lambda / \Delta x$
0.01	429.29	14.31
0.01	621.53	20.72
0.01	516.60	17.22
0.01	710.32	23.68
0.01	650.92	21.70
0.01	460.21	15.34
0.02	411.72	13.72
0.01	585.66	19.52
0.01	443.74	14.79
0.01	935.16	31.17
0.01	478.59	15.95
0.01	629.57	20.99
0.01	621.42	20.71
0.02	393.94	13.13
Average		18.78
Rounding Value		19

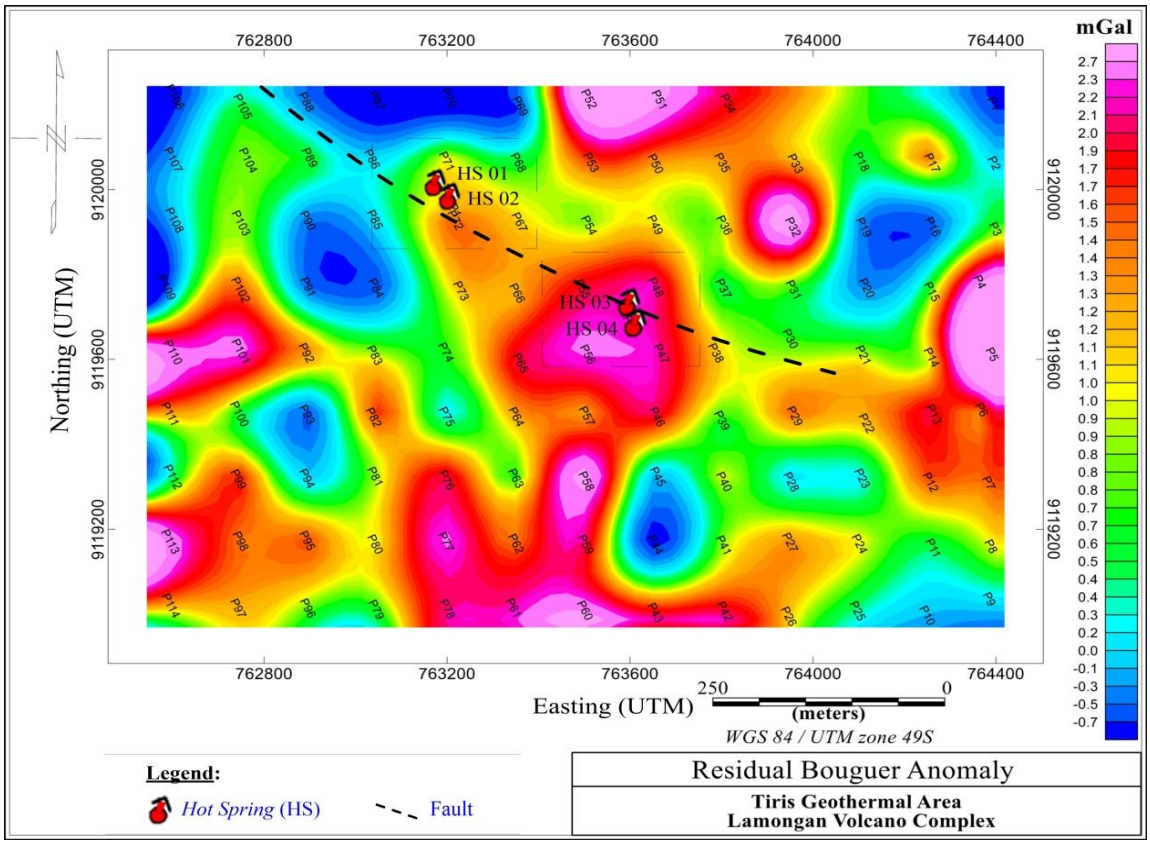

Fig. 12. Residual Bouguer anomaly map of the study area

3.6 Second Vertical Derivative

The second vertical derivative (SVD) method reveals and highlights local or shallow sources of anomalies [21]. This method can be used to determine the discontinuity of a subsurface structure, especially the presence of faults in a survey area [7]. The SVD anomaly map is the second derivative of the residual Bouguer anomaly by utilizing the SVD filter operator, namely the Elkins 5x5 matrix filter coefficient. The SVD map is shown in Fig. 13.

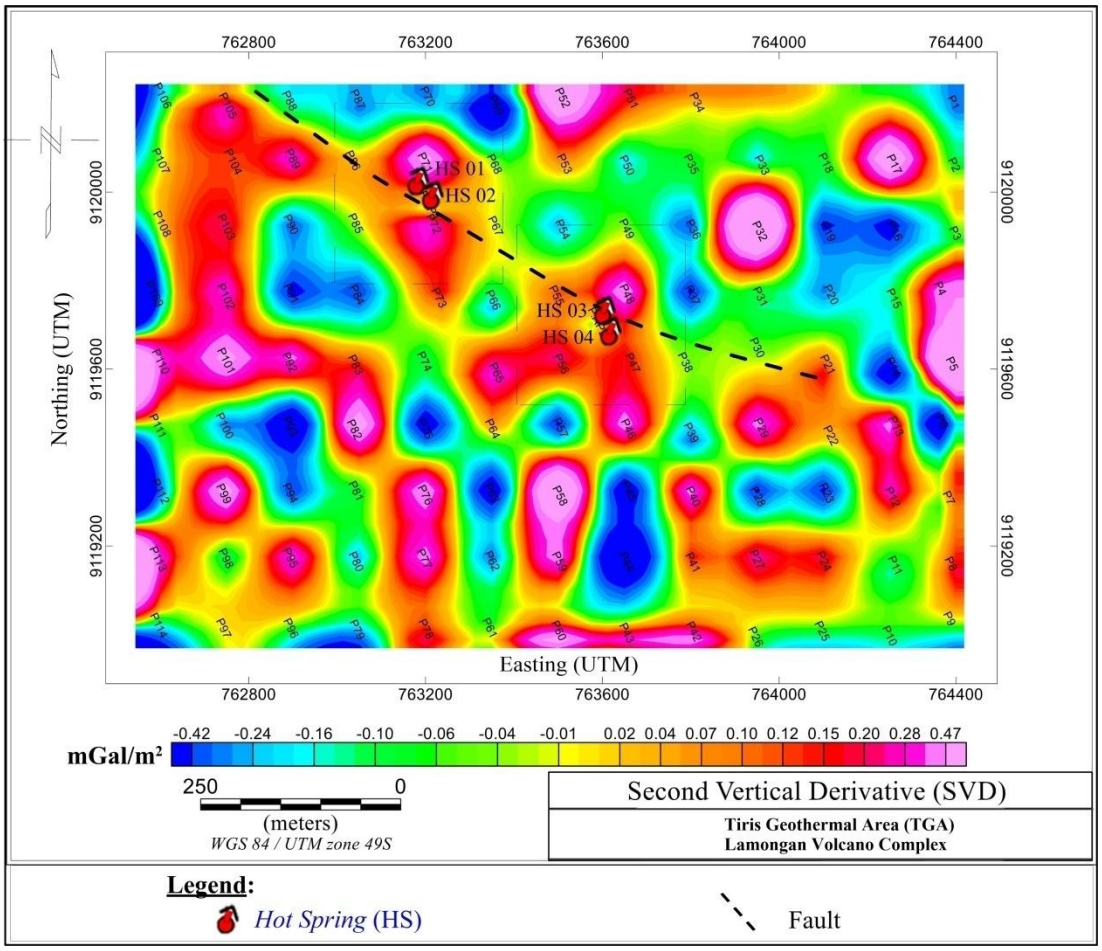

Fig. 13. Second Vertical Derivative (*SVD*) anomaly map of the study area

Fig. 13 shows that the SVD anomaly in the study area ranges from -0.42 mGal/m^2 to 0.47 mGal/m^2. Low SVD anomalies ranged from -0.42 mGal/m^2 to -0.01 mGal/m^2. Moderate SVD anomalies range from -0.01 mGal/m^2 to 0.12 mGal/m^2. Meanwhile, the SVD anomaly has a height ranging from 0.12 mGal/m^2 to 0.47 mGal/m^2. Low SVD anomalies were interpreted as low-density rock bodies, medium SVD anomalies were interpreted as medium density rock bodies, while high SVD anomalies were interpreted as high-density rock bodies. On the SVD map, the manifestation geothermal-1 and geothermal manifestations-2 are in the medium SVD anomaly, directly adjacent to the high anomaly. Contact boundaries between contrasting rock bodies, such as between high and low or medium density rock bodies, can be used to indicate the presence of weak zones like fractures or faults [7].

Based on the correlation between the SVD map and the geological map, it is found that the fault at the study area is northwest to southeast by breaking through the middle of a high-density rock body around the location where geothermal manifestations appear. This fault is thought to intersect the body of rock with high density around the Tancak river lane so that the direction of the fault continuity is not very clear.

3.7 Inversion Modeling

Inversion modeling is a form of modeling in which the model parameters are directly acquired from the processed data, which are automatically processed by the inversion algorithm in the ZondGM3D app. The 3D inversion modeling was performed using residual Bouguer anomaly data to get the subsurface density value. This modeling was conducted on approximately 2.16 km^2 with a target depth of ± 1111.13 meters below the acquisition points. The result of the 3D inversion modeling has an error value of 0.5%. The result of the 3D inversion modeling is shown in Fig. 14. Based on Fig. 14, there are two cross-

sections, namely the A-A' and B-B' cross-sections with a west-east direction with a track length of 1800 meters. Two cross-sections are cut just above the hot spring location. The two cross-sections are focused on the target to display the 2D slice shape of the subsurface geological structure just below the geothermal manifestation points. The primary purpose of making this cross-section is to interpret subsurface geological structures based on the distribution of density values. The two cross-sections of the 3D modeling of the study area are shown in Fig. 15.

Based on Fig. 15, the cross-sections A-A' and B-B' are composed of four rock layers. The four rocks are classified based on the distribution of density values in 3D inversion modeling and geological information of the study area. In addition, the interpretation and estimation of rock types from each subsurface constituent layer in the study area are also supported by several relevant previous studies related to geothermal systems in the Java island region. The first layer (blue) with a density (ρ_1) ranging from 2.52 $\mathrm{g/cm^3}$-2.67 $\mathrm{g/cm^3}$ is interpreted as lapilli tuff. This rock is one of the constituent rock types in the Lamongan volcanic rock formation. This lapilli tuff is a volcanic material resulting from the eruption of the Lamongan volcano [11]. This layer is very thin with a thickness of 50 m-200 m below the acquisition point and is assumed to be topsoil. The second layer (green) has a density (ρ_2) ranging from 2.72 $\mathrm{g/cm^3}$-2.77 $\mathrm{g/cm^3}$. The second layer is at a depth of 50 m-200 m below the acquisition point. The second layer is interpreted as tuffaceous breccia and is assumed to be cap rocks. Tuffaceous breccia is the result of a combination of breccia and clayey tuff rocks, and this rock layer can be interpreted as a caprock in the geothermal system due to the impermeable nature of clay [8,27]. The third layer (yellow-orange) has a density (ρ_3) ranging from 2.80 $\mathrm{g/cm^3}$-2.83 $\mathrm{g/cm^3}$, and is at a depth of 700 m-1000 m below the acquisition point. The third layer is interpreted as volcanic breccia rocks. The third layer is estimated to be reservoir rocks. This volcanic breccia is estimated to be the result of weathering of Lamongan Volcano basalt. This breccia consists of andesite, basalt, and a little

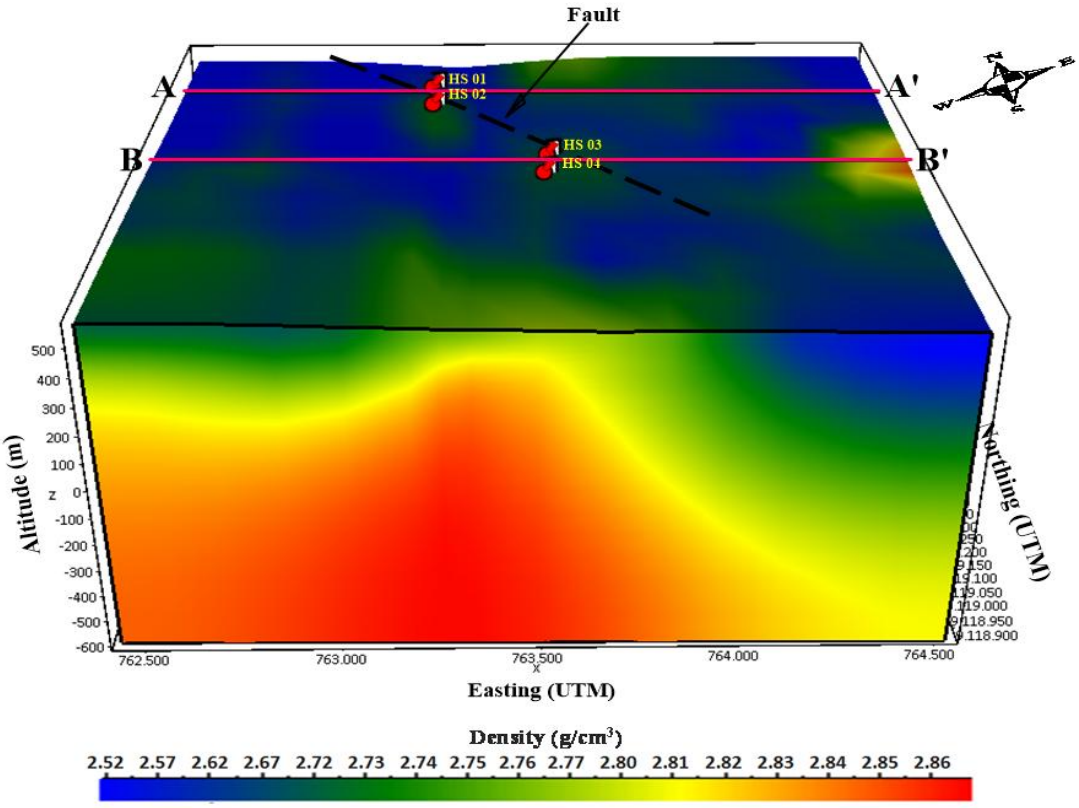

Fig. 14. 3D inversion modeling on residual Bouguer anomaly

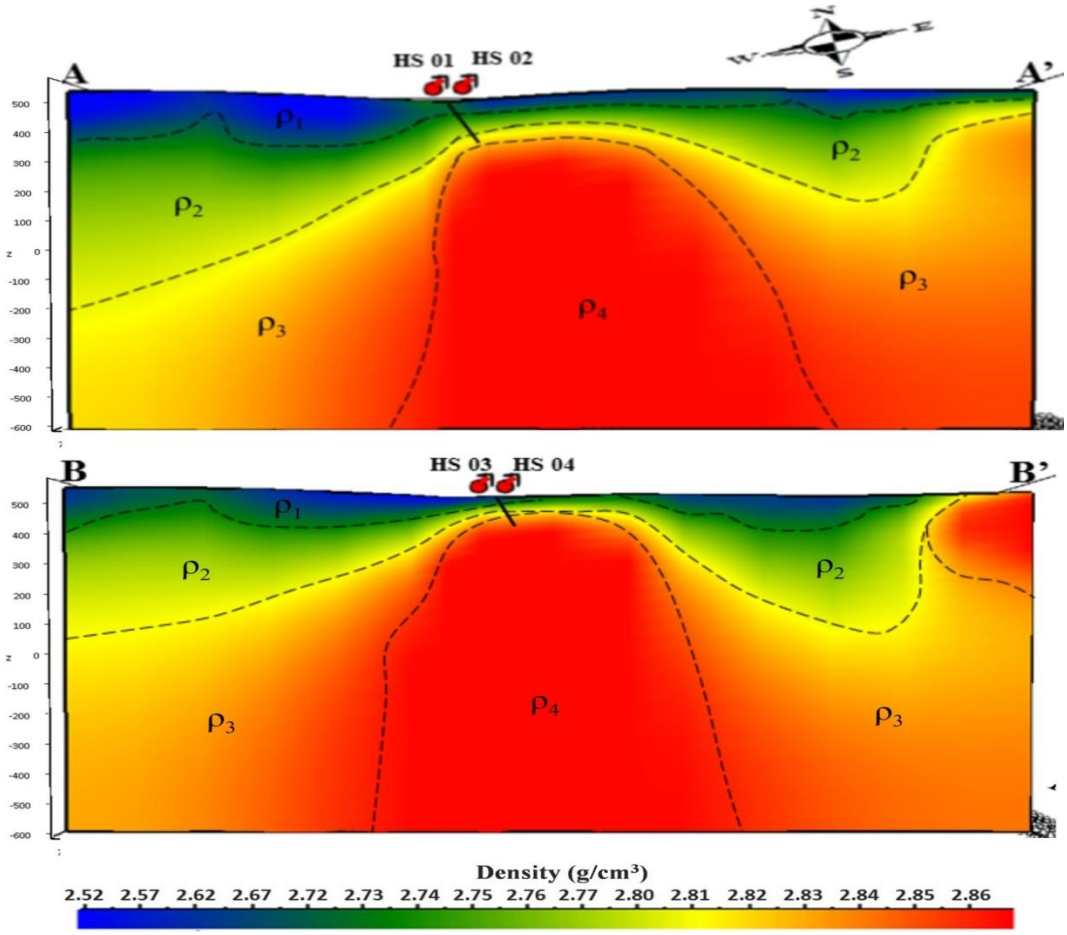

Fig. 15. A-A' and B-B' cross-section in 3D inversion model body

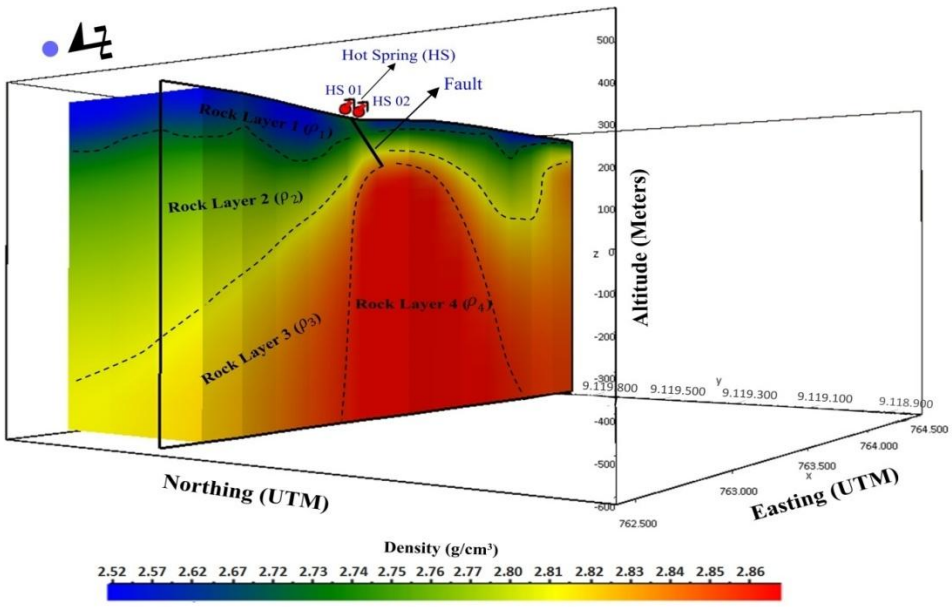

Fig. 16. Conceptual Model from 3D inversion of gravity data in the study area

pumice [11]. Breccia rocks are generally permeable and can pass fluids [8,28]. Based on previous research conducted by Maryanto et al. [5], it was found that the rock suspected to be a reservoir in the Tiris geothermal area is breccia rock. The fourth layer (red) has a density (ρ_4) ranging from 2.84 $\mathrm{g/cm^3}$-2.86 $\mathrm{g/cm^3}$ and is at a depth of 350 m below the acquisition point. The fourth layer is interpreted as basalt rocks in the form of intrusive igneous rocks. Intrusive igneous rocks generally have a high density. Several previous studies on geothermal fields and in potential mineral areas such as those conducted by Imam et al. [29], Susilo et al. [30], Azhari et al. [13], Wachidah & Minarto [31], obtained the density of intrusive igneous rocks which are quite high, respectively, namely 2.84 g/cm^3, 2.85 g/cm^3 and 3.30 g/cm^3. Intrusive rock can breakthrough because the rising magma undergoes very slow freezing, and the magma is volatile, which causes it to be pushed up so that it breaks through the surrounding rock because it finds fractures or weak areas in the rock [30]. This intrusive igneous rock can function as a heating rock for the surrounding reservoir rocks [30].

Based on the interpretation of the regional Bouguer anomaly map, the intrusive rock on the fourth layer of cross-section A-A' and B-B' is the dominant high anomaly pattern from the southwest towards the middle of the study area and right on the fault zone around the Tancak river. The southwest direction of the study area is the Lamongan volcano region. It is predicted that the intrusive rock, which is a high anomaly pattern on the regional Bouguer anomaly map, originates from the Lamongan volcano.

The result of the interpretation of the subsurface structure in the study area based on the 3D inversion modeling can be strengthened by the data from the estimated local density using the Parasnis method. The estimated local density value of 2.82 g/cm^3 illustrates that the rock structure at the study area is a massive volcanic rock structure. In addition, based on the spectrum analysis of the CBA map on a horizontal plane, it is found that the depth of the regional anomaly sources is 348 meters below the acquisition point. This analysis can be strengthened by the presence of intrusive igneous rocks at a depth of 350 meters below the acquisition point, as seen in Fig. 16.

4. CONCLUSION

The result of data processing shows that the CBA map on a horizontal plane has values ranging from 0.1 mGal to 4.2 mGal. Qualitative interpretation derived from the CBA map on a horizontal plane, the residual Bouguer anomaly map, and the regional Bouguer anomaly map, shows that there is a high anomaly in the middle of the study area, while a low anomaly dominates the northwest direction of the study area. The high anomaly at the study area is strongly suspected as intrusive rocks near the surface, while the low anomaly, which is dominant in the southwest direction, is suspected to be weak zones around the fault near the Tancak river. Quantitative interpretation is carried out by determining the local density of the study area, spectrum analysis, and cross-section on the results of 3D inversion modeling. The local density value according to the estimation using the Parasnis method is 2.82 $\mathrm{g/cm^3}$. This result is based on local geological information indicating that the subsurface condition of the study area is composed of volcanic rocks produced by the Lamongan volcano. The result of the spectrum analysis in the CBA on a horizontal plane shows the presence of a rocking body with a high density at a depth of 348 meters below the study area. Based on the cross-sectional view of the inverse 3D modeling results, it is found that the subsurface structure of the study area is composed of four main rock layers, sequentially from top to bottom, namely lapilli tuff, tuffaceous breccia, volcanic breccia, and basalt. This estimation and interpretation are based on the distribution of density values and local geological information. Based on the analysis of the subsurface structure, it is strongly suspected that the geothermal reservoir rock at the study site is volcanic breccia. This reservoir rock is in the third layer, with a depth of 700-100 meters below the study area. In addition, based on the cross-section view in 3D inversion modeling, it is strongly suspected that the fourth rock layer (basalt) is intrusive rock. This rock appears to be at a depth of 350 meters below the surface which tends to be in the middle of the study area. This estimation has positively correlated with the spectrum analysis result, which shows a regional anomaly source located at a depth of 348 meters below the study area. This intrusive rock is also suspected to be a heat source rock in the geothermal system in the Tiris geothermal area because it is a rock that originates from regional anomalies.

Future research is expected to use other geophysical methods with high penetration capabilities with the deeper span, such as magnetotelluric and seismic methods, to provide

accurate information about the geothermal system in the study area. In addition, this research still requires geological data such as borehole data to assist subsequent studies in interpreting the subsurface geological structure of the local area.

ACKNOWLEDGEMENT

The Authors thank the Geophysics Laboratory, Department of Physics, Faculty of Mathematics and Natural Science, University of Brawijaya, Malang, for assistance in collecting gravity data in the study area.

COMPETING INTERESTS

Authors have declared that no competing interests exist.

REFERENCES

1. Directorate of Indonesian Geothermal. Potential Geothermal Indonesia Vol. 1. Jakarta: Ministry of Energy and Mineral Resources; 2017.
2. Environmental Office of East Java. Environmental management performance Information of East Java Province year 2016. Surabaya, Indonesia.
   Accessed 6 May 2018
   Available:http://jatimprov.go.id/read/materi/informasi-kinerjapengelolaan-lingkungan-hidup-daerah-provinsi-jawatimur-tahun-2016
3. Deon F, Forster, HJ, Brehme M, Wiegand B, Scheytt T, Jaya M.S, and Putriani DJ. Geochemical/hydrochemical evaluation of the geothermal potential of the Lamongan volcanic field (Eastern Java, Indonesia). Geothermal Energy. 2015; 3(2):1-21.
   DOI: 10.1186/s40517-015-0040-6
4. Siombone SH, Maryanto S, Wiyono. Land Surface Temperature and Geomorphology of Tiris Geothermal Area, Lamongan Volcano Complex, Probolinggo, East Java, Indonesia. Environmental and Earth Sciences Research Journal (EESRJ). 2021;8(2):65-74.
   DOI: 10.18280/eesrj.080201
5. Maryanto S, Siombone SH, Prayogo A, Yulia T, Sari RPH. Preliminary study: Density layer values estimation of volcano hosted geothermal area at Tiris village, Probolinggo Regency, East Java, Indonesia. International Journal of Applied Engineering Research (IJAER). 2018; 13(6):4385-4390.
6. Telford WM, Geldart L, Sheriff RE. Applied geophysics, 2nd Editiond. UK Cambridge University Press; 1990.
7. Sarkowi M. Gravity Exploration, 1th edition. Yogyakarta: Graha Ilmu; 2014.
8. Hidayat N, Basid A. Gravity anomaly analysis as a reference in determining the subsurface geological structure and geothermal potential (case study in the Songgoriti area of Batu City). Jurnal Neutrino. 2011;4(1):35-47.
   DOI: 10.18860/neu.v0i0.1659
9. Raehanayati A, Rachmansyah A, Maryanto S. Study the potential of Blawan-Ijen geothermal energy, East Java based on the gravity method. Jurnal Neutrino. 2013;6(1):31-39.
   DOI: 10.18860/neu.v0i0.2444
10. Utama W, Riski S, Bahri AS, Warnna DD. Landsat ETM+ image analysis for the initial study determination of geothermal potential area at Mount Lamongan, Tiris, Probolinggo. Jurnal Fisika & Aplikasi. 2012;8(1):120103.
    DOI: 10.12962/j24604682.v8i1.858
11. Suharsono, Surwati T. Geological Map of The Probolinggo 1608-2 Quadrangle, Jawa (scale 1:100.000). Bandung, Indonesia: Geological Research and Development Centre; 1992.
12. Sunaryo. Identification of Arjuno-Welirang volcano-geothermal energy zone by means of density and susceptibility contrast parameters. International Journal of Civil & Environmental Engineering (IJCEE-IJENS). 2012;12(01):9-20.
13. Azhari AP, Maryanto S, and Rachmansyah A. Interpretation of Bouguer anomaly to determine fault and subsurface structure at Blawan-Ijen Geothermal Area. Jurnal Neutrino. 2016;9(1):1-9.
    DOI: 10.18860/neu.v9i1.3664
14. Parasnis DS. A study of rock densities in the English Midlands. Geophysical Journal International. 1952;6:252–271.
    DOI: 10.1111/j.1365-246X.1952.tb03013.x
15. Uwiduhaye Jd, Mizunaga H and Saibi H. Geophysical investigation using gravity data in Kinigi geothermal field, northwest Rwanda. Journal of African Earth Sciences. 2018;139:184-192.
    DOI: 10.1016/j.jafrearsci.2017.12.016
16. Lowrie, W. Fundamentals of Geophysics, University Press, 2nd Edition UK. Cambridge; 2007.

17. Dampney CNG. The equivalent source technique. Geophysics. 1969;34(1):39-53. DOI: 10.1190/1.1439996
18. Setyawan A. The mass point equivalent source method study in the process of gravity data lifting to a horizontal plane. Berkala Fisika. 2005;8(1):7-10.
19. Ashar MI, Irham MN, Danusaputro H. The subsurface modeling of the South West Java subduction zone is based on gravity anomaly data. Youngster Physics Journal. 2017;6(4):382-387.
20. Wahyudi EJ, Santoso D, Ulum AFM. Gravity Survey in Pandan Mountain – East Java, Indonesia. Journal of Physics: Conference Series. 2019;1204:012006. DOI:10.1088/1742-6596/1204/1/012006
21. Blakely RJ. Potential Theory in Gravity and Magnetic Applications, 1st ed. Cambridge: University Press; 1996.
22. Sumintadireja P, Dahrin D, Grandis H. A Note on the Use of the Second Vertical Derivative (SVD) of Gravity Data with Reference to Indonesian Cases. J. Eng. Technol. Sci. 2018;50(1):127-139.
23. Geological Agency, Ministry of Energy and Mineral Resources. Geothermal investigation book. Bandung: Center for Geological Resources; 2015.
24. Lewerissa R, Sismanto S, Setiawan A, Pramumijoyo S. The study of geological structures in Suli and Tulehu Geothermal Regions (Ambon, Indonesia) based on gravity gradient tensor data simulation and analytic signal. *Geosciences*. 2018; 8(1):4. Available:https://doi.org/10.3390/geosciences8010004
25. Nabighian MN, Ander ME, Grauch VJS, Hansen RO, La Fehr TR, Li Y, Pearson WC, Peirce JW, Phillips JD, Ruder ME. Historical development of the gravity method in exploration. GEOPHYSICS. 2005;70(6):113-139. DOI: 10.1190/1.2133785
26. Kearey P, Brooks M, Hill I. An introduction to geophysical exploration. 3rd edition. Paris: Blackwell Science; 2002.
27. Broto S, Putranto TT. Application of geomagnetic methods in geothermal exploration. Teknik. 2011;32(1):79-89.
28. Wangsa. A, Ismail N, Marwan. Quantitative interpretation of gravity anomaly data in geothermal field Seulawah Agam, Aceh Besar. J Aceh Besar Phys. Soc. 2018;7(1): 6-12.
29. Imam S, Supriyadi. Subsurface Structure of the Sekaran Area and Surroundings Based on Gravity Data. Unnes Physics Journal. 2014;3(1):42-46. ISSN 2252-6978
30. Susilo ND, Nurwidiyanto MI. Harmoko U. Subsurface interpretation with pseudo-gravitaty transformation based on geomagnetic data at the manifestation of kendalisodo hot springs, Semarang Regency. Youngster Physics Journal. 2016;5(4):195-202.
31. Wachidah A, Minarto E. Identification of Subsurface Structure of Potential Mineral Areas Using the Gravity Method at Field "A", Pongkor, West Java. Journal Sains dan Seni ITS. 2018;7(1):2337-3520. DOI: 10.12962/j23373520.v7i1.28673

Peer-review history:
The peer review history for this paper can be accessed here:
https://www.sdiarticle4.com/review-history/73468